SIMULATION OF GRAVIMETRIC CAPACITY, STRUCTURAL AND ELECTRONIC PROPERTIES OF VANADIUM DISULPHIDE AS ANODE MATERIAL FOR LITHIUM-ION BETTERY.

GLORIA ISENDI MURILA

A thesis submitted in partial fulfillment of the requirements for the Master degree of Science in Physics at Masinde Muliro University of science and technology

OCTOBER 2019

DECLARATION

This research thesis is my original work prepared with no other than the indicated sources and support and has not been presented elsewhere for a degree or any other award.

Signature..... Date.....

GLORIA ISENDI MURILA

SPH/G/23/2015

The undersigned certify that they have read and hereby recommend acceptance of Masinde Muliro University of Science and Technology a research thesis entiltled "Simulation of Gravimetric Capacity, Structural and Electronic Properties of Vanadium Disulphide as Anode Material for Lithium-ion Battery."

Signature..... Date.....

Dr George S. Manyali

Physics Department

Masinde Muliro University of Science and Technology

Signature..... Date .....

Dr Wafula Barasa Henry

Physics Department

Masinde Muliro Unviresity of Science and Technology.

COPYRIGHT

DEDICATION

This work is dedicated to my parents Mr. and Mrs. MURILA. Thanks a lot.

ACKNOWLEDGEMENT

First I would like to acknowledge God for His grace during my period of study.
I appreciate Dr. George S. Manyali (my supervisor), who introduced me to Computational Materials Science, allowed me to join his research group CTheP, guided me through all the steps of learning and working on my material of research.
Special regards to my mentor Dr. Henry Barasa. Right from undergraduate, you ensured that I got the best.

I acknowledge The Center for High-Performance Computing (CHPC), Cape Town, South Africa thanks for providing a HPC facility used in all calculations in this project. I also acknowledge support from Elkana Rugut of university of Witwatersrand South Africa for the dear support he offered during the entire project.

Special thanks to computational and theoretical physics group members (CTheP) for their valuable assistance in my course work and research. Finally my family members especially Murila Colvin I really acknowledge you.

MURILA G.I

ABSTRACT

Various energy sources are utilized at present with a challenge of energy storage in many cases. The existing rechargeable storage batteries which include sodium-ion and lithium-ion have some limitations in their gravimetric capacities. This can be improved by incorporating Vanadium disulphide (VS_2) due to its metallic properties at ground state. In this work we investigate the adsorption of lithium ions on the VS_2 layered material. Research shows that intercalating lithium ions on a monolayer VS_2 leads to a high energy capacity anode material but this has faced a challenge in obtaining the monolayer slab experimentally. For this reason, the *ab-initio* method based on density functional theory (DFT) was used to investigate the adsorption of lithium ions on layered Vanadium disulphide with no bonds in the positive electrode being broken. All calculations were done within the DFT framework and a plane wave basis set as implemented in Quantum Expresso code. The projector augmented wave (PAW) pseudo potentials were used to describe the electron-electron interaction. From the calculation H-phase monolayer VS_2 was found to be stable at room temperature maintaining the hexagonal structure. Also pure and lithium adsorbed VS_2 was found to be electronically stable with zero band gap thus the metallic state is maintained upon intercalation. VS_2 gives a maximum gravimetric capacity of 466mhA/g showing that it offers a more favorable adsorption sites for lithium atoms. With the structural and electronic stability of VS_2 coupled with a high gravimetric capacity, VS_2 is an effective anode material for a high storage capacity lithium ion battery. Thus can be applied in electrical devices.

Table of Contents

LIST OF TABLES

LIST OF FIGURES

ACCRONYMS AND ABREVIATIONS

VS_2	Vanadium disulphide
LiBs	lithium ion betteries.
3D	Three dimension
2D	Two dimension,
PBE	Perdew Burke Ernzerhof.
PW	Plane Wave.
VESTA	Visualization for Eectronic and STuctural Analysis
CAS	Compressed Air Storage
HAS	Hydroulic Accumulates.
FES	Flywheel Energy Storage.
DOS	Density of States.
TPS	Tao-Perdew-Stravovevor-Scuseria.
H	Hamiltonian operator
E_{ga}	Band gab energy.
GGA	Generalised Gradient Approximation.
∇	Gradient operator.
$n(r)$	Electron charge density.
V_{ext}	External potential,
$F[n(r)]$	Functional of density.
E_{cut}	plane wave cut off energy.

PDOS	Partial Density of States.
FL-LAPW	Full Potential Linearized Augmented Plane Wave
NEB	Nudged-energy path
MEP	Minimum-energy path.
MT	Muffin-tin
PAW	Projector Augmeted Wave
ESS	Energy Storage System
LTMD	Layered Transtional Metal Dichalgogenides.

CHAPTER ONE

INTRODUCTION

1.1 Energy Storage

The primary energy sources such as coal, natural gas and petroleum have been in use for many years. These form of energies are classified as non-renewable energy sources. Overreliance on these sources of energy leads to environmental problems due to the way they are extracted and processed or in terms of how they are used and therefore disposed of. Some of the effects of non-renewable energy includes: increase in the amount of greenhouse gases in the air, emission of mercury from coal-fired plants, acid rain and water pollution among others.

This has led to a rising concern of environmental pollution. To overcome these, renewable energy sources has to be placed in position. Research has been carried out on other sources of energy such as wind, wave and solar (Goodenough & Kim, 2009). These renewable resources are usually interminet since they are affected by weather and geographical regions. For better utilization of such energy sources, energy storage systems (ESSs) are a key factor (Zhenguo, et al., 2010).

Typically, most current energy storage technologies are based on the conversion of chemical energy into electrical and light energy where energy is stored in the form of chemical potential. Batteries have high conversion efficiency and due to the advantages of long cycle life and relatively low maintenance, they are the most utilized ESSs (Yu-Guo, *et.al.,* 2008). Rechargeable Lithium-ion batteries have been widely used in most consumer electronics which includes: cell-phones, personal

digital assistance, cameras, laptop computers and electric vehicles. Engineers have all along been devising methods in designing light and portable electronic machines which depend on these batteries as the power bank. In recent years Nanostructured compounds used as batteries' electrodes materials have been on the fore front in most research work (Maier, 2005).

The challenge has been coming up with batteries that have high energy storage capacity (Tarascon & Armand , 2001). For instance, the current Li-ion batteries used for the Nissan Leaf can only support 50-100 miles per charge (Larramona, *et al.*, 2006). Major researches have been conducted on the electrode materials of rechargeable batteries to address this problem. The most researched on is the Lithium-ion battery since it has most attractive merits such as higher voltage, higher energy density, and longer life cycle. Other rechargeable batteries like lead acid accumulators and Nickel-Cadmium batteries lack the above properties which hinders their applicability. Despite their positive success the available lithium ion batteries cannot meet the high energy demand.

1.2 Metal Chalcogenides.

Nano-materials are on the forefront in most studies of anode materials. Chalcogenides with molecular formula MX_2 (where M is the transitional element and X the chalcogenide which include elements like Sulphur, Selenium, Tellurium and Polonium), have attracted high attention because of their high surface areas, active edges state and high mechanical flexibility. Transition metals mostly used includes (Mo, W, and V). One layer of the transitional element atoms is sandwiched between two layers of the Chalcogenides atoms. They are part of the large new family of the

so called 2D materials. Most of these materials in this family are semiconductors with a small band gap of around 1eV - 2eV which limits their electrochemical performance (Yu, *et.al.*, 2014). Also the high molecular weight limits lower the gravimetric capacity (Wenhui, *et al.*, 2016).

However, layered transitional metal Sulphide are considered as the promising electrode material due to their outstanding electron behavior, large surface area and high chemical tolerance (Jian-Zhe & Peng-Fei, 2015). Vanadium disulphide (VS_2) is a unique compound of the existing transitional metal dichalcogenides.

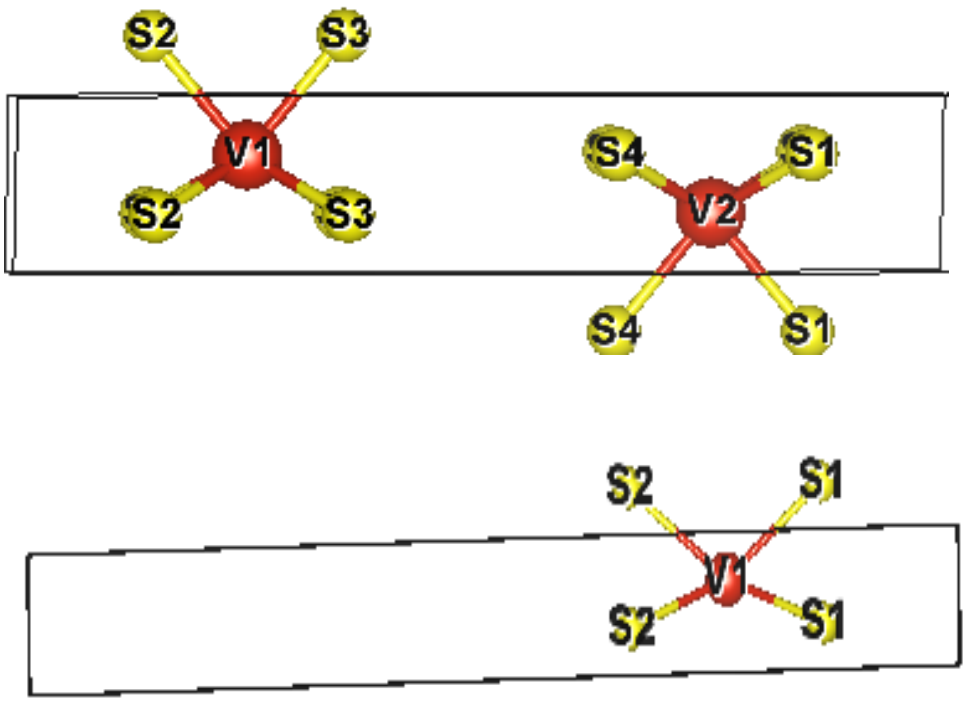

Figure 1.1: (a) Bulk and (b) Monolayer system of Vanadium disulphide (Yellow and maroon balls represents Sulphur and Vanadium atoms respectively).

The bulk stable structure of VS_2 is made up of vanadium atom surrounded with two Sulphur atoms throughout the hexagonal structure. The bulk system is thus made up of three layers of VS_2 bounded to each other by an approximated distance of 0.64nm. Van der Waals force held the monolayer planes together. To achieve a monolayer slab the lateral axis is exfoliated by creating a vacuum of about 20 Å

1.3 Statement of the Problem

Layered Metal dichalcogenides (LTMDs) have aroused a special interest among researches due to their ability to be used as positive electrode materials in both Lithium-ion batteries (LiBs) and Sodium-ion batteries (SiBs) (Yu-Guo, *et al.,* 2008). Many of these materials that have been studied includes metals like Molybdenum (Mo), Tungsten (W), Tin (Sn), and Titanium (Ti) together with their chalcogen atoms like Sulfur (S) Selenium (Se) and Trillium (Te) (Xiao, *et al.*, 2016). The LTMDs have shown to be promising candidates for battery applications in most reported research though the gravimetric capacity is still low (Feng, *et al.,* 2014). This is as a result of most of them being semiconductors in monolayer state which limits their electrochemical performance like electrochemical stability and poor binding ability and poor electron transport. The higher molecular weight of most LTMDs leads to low gravimetric capacity. This leads to cracking of electrodes and thus reduced life span of the battery. To address these, the research is geared towards predicting an alternative LTMD that maintains the metallic state in both bulk and monolayer state and has low molecular weight hence high gravimetric capacity through *ab initio* methods.

1.4 Objectives

1.4.1 Main Objective of this Study

To determine gravimetric capacity, structural and electronic properties of monolayer VS_2 as an anode material for Lithium-ion batteries applications.

1.4.2 Specific Objectives

I) To determine the structural properties of VS_2 in 3D and 2D state

II) To determine the electronic properties of a pure monolayer VS_2 and lithium adsorbed VS_2.

III) To calculate the gravimetric capacity of monolayer VS_2 adsorbed with Li-ions.

1.5 Justification.

This research predicts an electrode with high gravimetric capacity through intercalation of lithium ions by *ab initio* methods. The electrode must have the capability to change the valence states, space to accommodate Li-ions and maintain a reversible exothermic reaction during the intercalation. Semi-metallic VS_2, which is a member of TMDs is thus assumed to address this issue. VS_2 has a low molecular weight of 50.9415amu, with three possible site for lithium accommodation. It also has high negative adsorption energy upon intercalation with a low lithium diffusion barrier and a low average open circuit voltage of 0.93V (Jing, *et al.*, 2013). Ab initio methods will be employed in this research due to their accuracy and detailed properties that they give. The results in this study will guide the experimentalist in coming up with an electrode material that can lead to high gravimetric capacity battery.

1.6 Scope of this Study

Gravimetric capacity, structural and electronic properties of a pure monolayer VS_2 as well as when lithium ions are adsorbed on its surface were covered. All parameters characterized using *ab initio* method. This study only considered the composition of the anode material.

CHAPTER TWO

LITERATURE REVIEW

2.1 Introduction

There is high rate of environmental pollution currently. This is as a result of over reliance on non-renewable energy sources due to high energy consumption. The best way of dealing with this issue is to make use of renewable and clean energy sources. This can only be useful with proper energy storage mechanism in place.

Globally, energy storage is on the fore front (Liu, *et al.*, 2010). An energy storage device is one of the apparatus used for storage of electric energy to be used when need arises. It works on the basis of converting energy from non-energy storage sources to a conveniently and economically storable form. Energy storage systems date back to ancient times where the process was simply natural (Kibuuka, *et al.* 1991) at this time storage mechanism were not fully developed.

2.2 Energy Storage Technology

Energy storage is a measure to counter global warming, with the main aim of curbing environmental pollution. This is the most important role in production and utilization of energy. Energy storage technology is of different types. Some of these energy storage methods includes:

I. Mechanical storage.

In mechanical storage, energy is stored in water, pumped at a higher elevation using pump storage methods. Mechanical storage capacity can be of different forms for

example compressed air storage (CAS), hydraulic accumulators (HAS) and fly wheel energy storage (FES) devices among others.)

II Thermal storage

Thermal energy storage materials are compounds or mixtures that reversibly undergo modification or change of state with accompanied release of latent heat. They include brick storage heater, solar pond steam accumulator (Hasnain, 1998). The energy stored in these devices is extracted by direct contact with heat interchange fluid. The fluid is chemically inert to the composition in order. Thermal storage is a temporary storage method.

III Electrical energy storage

This storage technology is classified into three major categories. They include Flywheel and super capacitors, geological storage and battery storage technology. These technologies are large-scale with high energy storage (Hall & Bain, 2008). Despite these merits, electrical storage technologies require special terrain and have large capital investment and maintenance costs.

2.3 Batteries

A battery is an electrochemical cell that can be charged electrically to provide a static potential for power or released electrical charge when needed. Batteries are made of series of cells that produce electricity. With three essential components: (i) anode (ii) cathode, and (iii) electrolyte. A connection of an anode and cathode via an electrolyte, leads to a flow of electrons from the anode to the cathode (Tarascon & Armand , 2001)

The characteristic of a given battery is determined by the components of each cell, which includes gravimetric capacity and output voltage. Chemical energy determines the total gravimetric capacity a battery can store. Batteries are classified as rechargeable and non-rechargeable batteries. A rechargeable battery has one or more electrochemical cells combined together. These batteries electrochemical cell reactions are reversible and thus the name secondary cell (Wu, *et al.*, 2014). They are the most commonly used due to their differences in shape and size.

The initial cost of these batteries is usually high but the cost is lower during recharge. In comparison to non-rechargeable batteries, rechargeable batteries are environmentally friendly. The common rechargeable battery types are tabulated in table 2.1 below.

Table 2.1: Types of rechargeable batteries

Types of batteries	Properties	Example of uses	Advantage.
Sealed Lead Acid batteries	High charge for duration of three years.	For backing up emergency power sources	Less expensive
Nickel Cadmium batteries	High charge and energy discharge rate	Popularly used in electrical toys and video equipment	Cheap and widely used.
Nickel-Metal Hydride (Ni-MH) battery	Output voltage of 1200V and capacity of 1500mAh.	Portable computers; cellular phones; same as for Ni-Cd batteries	It is not affected by memory loss therefore no self-discharge
Lithium-ion batteries.	It is the most stable rechargeable battery with the highest gravimetric capacity	Commonly used in consumer electronics like lap-tops, mobile phones	It has more charge than all Other batteries. It exhibits a low self-discharge.

Storage capacities can be increased through, a combination of number of inorganic compounds with reversible chemical reactivity with alkali metals. This is done through intercalation reaction. Most electrode reactions in batteries are intercalated reactions (Nitta, *et al.*, 2015). Lithium or sodium ions are introduced into a host electrode with no change in original structure. Increasing the gravimetric capacity of the current lithium batteries is the major research area today.

2.4 Lithium Batteries

Lithium ion batteries are a type of rechargeable battery which provides energy through a reversible reaction. The battery gives out power during discharge and it absorbs power during charging (Xin-Bing, *et al.,* 2018). The main components of the batter are the electrodes (anode and cathode) and the electrolyte. The common electrolyte used is a Lithium salt like Lithium hexafluorophosphate ($LiFP_6$) (Vadim, *et al*., 2015) which is a polar substance and highly soluble, releasing Li-ions in aqueous state. Lithium-ion batteries commonly use intercalated compounds as anode materials. The figure below shows a cross sectional lithium –ion battery.

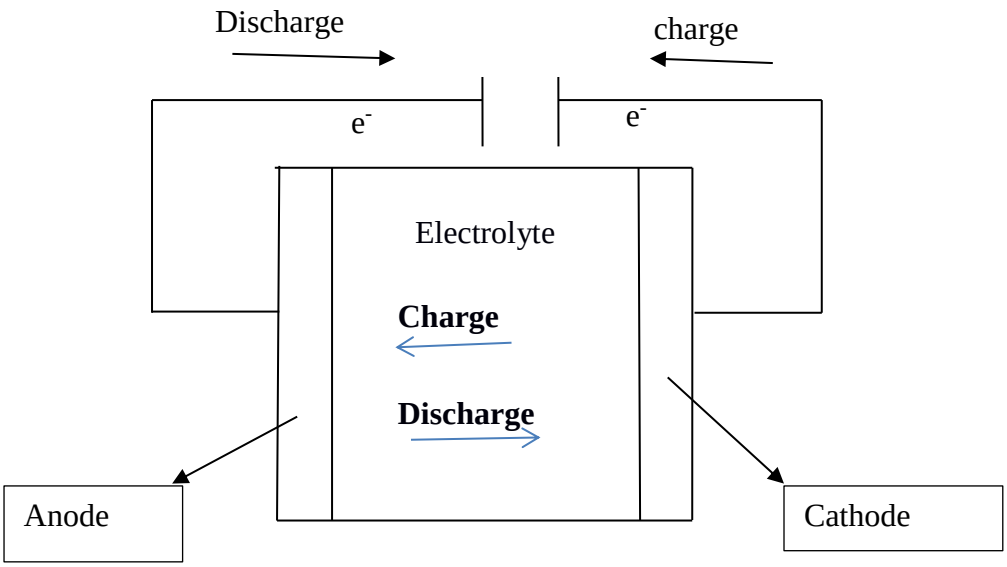

Figure 2.1: Cross section of lithium ion battery.

The figure shows a cross section of lithium ion battery. The cathode and anode are separated by an electrolyte. The transfer of Lithium-ions between the electrodes is facilitated by the electrolyte.

During discharge lithium ions intercalate into the cathode providing an electric current. The cathode becomes more positive and this attract electrons which flows in the outer circuit via our device toward the cathode. On charging the Lithium ions flows to the anode as the battery stores energy.

Generally, lithium is preferred because it can be easily handled (though with care) as compared to other alkali metals (Placke, *et al.,* 2017). Lithium is a light metal and highly electropositive. It has a low density of $0.534g/cm^3$ leads and hence high gravimetric capacity of 3.86Ah/g (Raji, *et al.,* 2017). When compared with other alkali metals. For this reason, lithium batteries are highly applicable in most electronic devices.

2.4.1 Anode Materials.

In 1960s John Goodenough proposed the first LiBs. His ideas were advanced by Stanley Whittingham in 1990s. His first LiBs were made up of lithium metal Titanium (IV) Sulphide as the electrode. This battery was the most expensive in the market then. Apart from its high cost, this battery had a low energy capacity and it was not environmental friendly. For example, when the Titanium disulphide reacts with air, it forms hydrogen compounds which have a bad odor. Silicon seemed to be the best anode material to be used. It had a high energy potential of 4200mAh/g. However, it was limited by high expansion and contraction during charging and discharging (Etachari, *et al.,* 2011). This makes the electrode to crack and lose contact with electronic current collector thus reducing the life cycle of the battery (Sakuda *et al*.,

2008). Other materials such as tin and silicon oxide SiO_2 were also adopted. Their energy capacities were 994mAhg and 782mAhg respectively. Despite the high energy capacity, the applicability of these materials is mostly affected by their poor cycling behavior which results from large volume changes on progressive alloying process with lithium ions. Later lithium electrodes were adopted. Its theoretical specific and volumetric capacity is found to be 3829mAh/cm^3 and 2044mAh/cm^3 respectively (Guduru & Leanza, 2016) .The use of lithium electrodes also faced lots of challenges. For instance lithium is a very reactive metal and it burns vigorously at normal temperature-pressure conditions when exposed to oxygen. Metal electrodes having failed researchers opted for intercalated anode materials.

2.4.2 Intercalated Anode Materials.

To eliminate the problem of poor lithium rechargeable and increase safety aspects of high energy storage battery, there is need of intercalated anode material. Initially in 1990s, efforts were made by several researchers including Gregory and Novak on electrochemical insertion of Mg^{2+} into various metal oxides and sulfide of different transitional metals (Novak, *et al*., 1994).

This work was successful though research shows that there was a screening effect of water on Mg^{2+} during the intercalation processes (Novak, *et. al.,* 1995). This opened ways and interest for different scholars to research on intercalations behavior of polyvalent ions in various electrode materials with reference to sodium and lithium batteries. Research shows that intercalated anode materials in lithium batteries started with graphite with low energy capacity of 372mAh/g (Trevey, *et al.,* 2009). Due to its low energy capacity silicon was adopted. It had the highest energy capacity of 4200mAh/g with operating voltage of 0.4V. Intercalation reaction requires that the host electrode materials should possess space to accommodate Li-ions as well as

neutrality. The most appropriate and widely researched materials are transitional metal oxides and Sulphide which have layered-like structures (Chaofeng, *et al.,* 2016).

2.4.3 Layered Transitional Metal Dichalcogenides Anode Materials (LTMDs)

LTMDs have large surface area and variable oxidation state which allows electrically double layer reversible oxidation-reduction reaction for charge storage mechanism. Monolayers TMDs exhibits high electrochemical activity derived from its edge sites which offers high storage capacity (Choudhary, *et. al.,* 2016) Molybdenum disulphide (MoS_2) is an example of LTMD that has been explored extensively. It exhibits good electrochemical potential with lithium ions intercalating very well on its layers (Wenpei, *et al.,* 2017). However the electrochemical performance is limited by its semiconducting behavior in 2D state (Yu, *et al.*, 2014). As a semiconductor it has poor electron transport efficiency (Jian-Zhe & Peng-Fei, 2015). Furthermore, Molybdenum is a heavy metal and highly electronegative that leads to strong covalent bonds with Sulphur within its structures. Vanadium disulphide nano-sheets can be obtained experimentally through exfoliation using ammonia (Feng, *et al.,* 2011). Each layer is made up of hexagonal close-packed sheets of Vanadium atom surrounded by the Chalcogenides of Sulphur atoms. Interlayer bonds are covalent while the intralayer is stacked by Van der Waals forces. The interlayer spacing is roughly 6.15 Å which are very large making the compound to undergo rapid change in volume during expansion upon lithium storage. It also mitigates the strain endured in the intercalated or reversible reaction leading to enhanced cycling stability.

Compared to MoS_2, VS_2 monolayer is metallic with spin-polarized ground state (Ma, *et al.,* 2012). In addition, metallic VS_2 could facilitate good performance in Li-ion battery as an anode. In this research we performed a systematic DFT computation to explore the possibilities of using VS_2 monolayer as anode material for LiBs.

CHAPTER THREE

THEORETICAL FRAME WORK

3.1. Introduction

First principle Computation is becoming the way to go in exploring features of most compounds. This makes it possible to understand the compound's structures and easily determine its behavior. The computations are usually a representation of calculated models of systems structure to get to understand its application and to estimate its performance. In this section fundamental theories supporting the study both at ground state and excited state are discussed.

The improvement in the scope and range of studying solid state physics, upgrading from semi-empirical descriptions based on qualitative models to thorough systematic analysis of quantitative physical properties formed the basis of this work. The work was based on the quantum mechanical description systems as made of interaction of electrons in the field of atomic nuclei otherwise known as First Principles or *Ab-initio* Calculations (Ponomaranko, *et al.,* 2008).

The Schrödinger equation forms the basis for all quantitative calculations for solid state properties. Here, the Hamiltonian for any such system is considered to be composed of the kinetic energy T, of the particles of the system as well as the electron and nuclei interaction energy or the potential V, of the system. The reason for the success of computational methods lies in the original reformulation of the Schrödinger equation to Kohn-Sham equations coupled with the physical insight of the correlation effects of interacting electrons in the vicinity of a slowly varying field (Mueni, 2012).

3.2 Many Body Perturbation Theory

It provides a convenient framework for calculation of interactions between electron–electron nuclei (Manyali, 2013) .The general Hamiltonian H, for many body system is given by

$$H = \sum_i \frac{-\hbar^2}{2m_i} \nabla_i{}^2 + \frac{1}{2}\sum_{ij} \frac{Z_i Z_j e^2}{(\vec{R}_i - \vec{R}_j)} - \sum_k \frac{\hbar^2}{2m_e} \nabla^2{}_{rk} + \frac{1}{2}\sum_{kl} \frac{e^2}{(\vec{r}_k - \vec{r}_l)} - \sum_{k,l} \frac{Ze^2}{(\vec{r}_k - \vec{R}_l)}. \quad 3.1$$

Where;

$\sum_i \frac{-\hbar^2}{2m_i} \nabla_i{}^2$, describe the electronic kinetic energy (T_e)

$\sum_{ij} \frac{Z_i Z_j e^2}{(\vec{R}_i - \vec{R}_j)}$, is the repulsive term due to nuclei-nuclei interaction, (V_{nn})

$-\sum_k \frac{\hbar^2}{2m_e} \nabla^2{}_{rk}$, is the nuclei kinetic energy(T_n)

$\sum_{k,l} \frac{Ze^2}{(\vec{r}_k - \vec{R}_l)}$, is the nuclei potential acting on the electron interaction (V_{ee})

$\frac{1}{2}\sum_{kl} \frac{e^2}{(\vec{r}_k - \vec{r}_l)}$, describe the repulsive force from ion-ion interaction (V_{ne})

Considering these the Hamiltonian can be written as:

$$H = T_e + V_{nn} + T_n + V_{ee} + V_{ne}. \quad 3.2$$

To solve this equation some approximations are employed, Born-oppenheimer (B-O) approximation is one of the solution to this problem. In this approximation, the nuclei are assumed heavier in comparison to the charge carriers (electron). The nucleus is taken as a stationary body while electrons are in motion. The full wave-function (ψ) which is assumed to be a function of the electron position, r_i and nuclear position, R_l written as;

$$\varphi(r_i, R_l) = \emptyset(r_i, \{R_l\})X(R_l). \quad 3.3$$

Where:

$\emptyset(r_i, \{R_l\})$: is an electron wavefuction whose parameters are dependent to the nuclear position.

$X(R_l)$, is the electron state for the fixed nuclear configuration$\{R_l\}$. This is the solution to the vibrational problem for the nuclear coordinates in the presence of an electronic potential energy surface.

3.3 Hohenberg-Kohn Theorem

It formulates the DFT as being a true theory of many body systems (MBS). Considering a number of unknown volume of electrons enclosed in a given box with a mutually influenced columbic repulsion with some external potential V (r), then the Hamiltonian will be expressed as;

$$H = T + V = \frac{1}{2}\nabla\varphi^*(r)dr + \int V(r)\,\varphi^*(r)\varphi(r)dr +$$

$$\frac{1}{2}\int \frac{1}{|r-\acute{r}|}\varphi^*(r)\,\varphi^*(\acute{r})\varphi(\acute{r})\varphi(r)dr. \qquad 3.4$$

The electron density at the ground state n(r) that depends on the external potential V(r) is defined as;

$$n(r) \equiv \langle \varphi \vee \varphi^*(r)\varphi(r) \vee \varphi \rangle \qquad 3.5$$

Assuming a non-degenerate ground states which suggest that two or more different states of a system cannot give the same value of energy upon measurement. A *reduction-ad absurdum* is then applied to show that V(r) is a unique function of n(r).We assume that there also exists another ground state $\grave{\varphi}$ that gives rise to the same electron density n(r); unless $\grave{V}(r) - V(r)$=constant; $\grave{\varphi}$ and φ are non-equal as they satisfy independent Schrödinger equations. When ground state energies and Hamiltonian are denoted as with φ and $\grave{\varphi}$ by E, É and H, $\grave{H}$ in that order, the minimized ground state expression obtained is as follows:

$$H = T + U_{el} + V_{ext} \Rightarrow H\varphi = E\varphi. \qquad 3.6a$$

$$\grave{H} = T + U_{el} + \grave{V}_{ext} \Rightarrow \grave{H}\grave{\varphi} = E\acute{\varphi}. \qquad 3.6b$$

From variation principle, starting from É we get;

$$E = \left\langle \varphi \acute{\vee} \acute{H} \vee \acute{\varphi} \right\rangle < \langle \varphi \acute{H} \varphi \rangle. \qquad 3.7$$

Assuming É is the ground state energy then;

$$\langle \varphi \vee H \acute{\vee} \varphi \rangle = \langle \varphi \vee H - V_{ext}(r) + \acute{V}_{ext}(r) \vee \varphi \rangle = E + \int drn(r)\left[\acute{V}_{ext}(r) - V_{ext}(r)\right]. \qquad 3.8$$

Integrating raised and unraised functions of the equation 3.8, we get;

$$\acute{E} < E + \int drn(r)\left[\acute{V}_{ext}(r) - V_{ext}(r)\right]. \qquad 3.9$$

Also starting from E, we get;

$$E = \langle \varphi \vee H \vee \varphi \rangle < \langle \acute{\varphi} \vee H \vee \acute{\varphi} \rangle = \acute{E} + \int drn(r)\left[\acute{V}_{ext}(r) - V_{ext}(r)\right]. \qquad 3.10$$

Following this assumptions, n(r) =$\acute{n}$(r), where $\acute{n}$(r), ground state charge we get from $\acute{H}$ which has a ground state energy of $\acute{E}$ that results in;

$$E < \acute{E} + \int n(r)\left[V_{ext}(r) - \acute{V}_{ext}(r)\right]. \qquad 3.11$$

Summing (3.9) and (3.10) a contradicting inequality that results is:

$$E + \acute{E} < E + \acute{E}. \qquad 3.12$$

From the above equation Pauli Exclusion Principle is confirmed (Hohenberg, 1964), In addition the same explanation can be applied to degenerate ground state with more ground states.

3.4 The Hartree-Fock Approximation Approach

In this theory electrons are assumed to be in contact with each other. In this case Hamiltonian is written as:

$$H = \sum_{\alpha}^{N} h_{\alpha}. \qquad 3.13$$

Where: h_{α} is the total kinetic and potential energies of one electron of any given atom. This wave function is associated to the new Hamiltonian (called Hartree-product) and is given by the equation:

$$\emptyset(x_1, x_2, x_3, \dots \dots \dots x_N) = \varphi_1(x_1).\varphi_2(x_2).\varphi_3(x_3) \dots \dots \dots \dots \dots \varphi_N(x_N). \qquad 3.14$$

Where x_1 is a generalized coordinate that incorporates the spatial and spin degree of freedom. For this equation, the energy of one electron in the spin orbital j is given as: $\psi\varphi\psi\Psi$

$$h_j\varphi_j(x_i) = \epsilon_j\varphi_j(x_i). \qquad 3.15$$

Therefore, to get the total energy, we sum the energies of all the electrons and this results;

$$\langle\emptyset(x_1, x_2, x_3 \dots x_N)|H|\emptyset(x_1, x_2, x_3, \dots x_N)\rangle =$$

$$\sum_{i,j}^{N}\langle\emptyset(x_1, x_2, x_3 \dots x_N)\left|h_{jk}\right|\emptyset(x_1, x_2, x_3 \dots x_N)\rangle = \epsilon_1+\epsilon_2+\epsilon_3+\dots+\epsilon_N = E \quad 3.16$$

This model failed because it could not explain clearly the Pauli Exclusion Principle. According to this principle the wave function of the fermions must be anti-symmetric in relation to particle exchange. Thus to build an anti-symmetric wave function, fermion-system should be incorporated when dealing with Hartree wave function. The possible wave function used in this case is called slater determinant which is an anti-

symmetric wave function. In this description, N-electron system has a determinant of N X N matrix of the one electron wave function.

$$\emptyset(x_1, x_2 \dots, x_N) = \frac{1}{\sqrt{N!}} \begin{vmatrix} \psi_{1(x_1)} & \psi_{2(x_1)} & \dots & \psi_{N(x_1)} \\ \psi_1(x_1) & \psi_2(x_2) & \dots & \psi_N(x_2) \\ \vdots & \vdots & \ddots & \vdots \\ \psi_{1(x_N)} & \psi_2(x_N) & & \psi_N(x_N) \end{vmatrix}. \quad 3.17$$

For illustration, consider the two electron system, equation 3.17 then becomes

$$\emptyset(x_1, x_2) = \frac{1}{\sqrt{2}}[\psi_1(x_1)\psi_2(x_2) - \psi_1(x_2)\psi_2(x_1)] \quad 3.18$$

From these electrons we get a wave function given by the equation:

$$\emptyset(x_2, x_1) = \frac{1}{\sqrt{2}}[\psi_1(x_2)\psi_2(x_1) - \psi_1(x_1)\psi_2(x_2)] = -\emptyset(x_1, x_2). \quad 3.19$$

These elections when placed in the same state therefore

$$\emptyset(x_1, x_1) = \frac{1}{\sqrt{2}}[\psi_1(x_1)\psi_2(x_1) - \psi_1(x_1)\psi_2(x_1)] = 0. \quad 3.20$$

This indicates that the slater determinant matrix is an exact wave-function of N, non-interacting, single particles moving in the field of the effective potential experienced by an electron due to the effective potential V_{HF} which is the average repulsive potential experienced by an electron due to the $(N-1)$ other electrons and the nuclei. Thus the Hartree-Fock equation is given by

$$\left[-\frac{1}{2}\nabla_i^2 + \sum_K^n \frac{1}{|R_K - r_i|}\right]\psi_\alpha(r_i) + \left[\sum_\beta^{occ} \int dr_j \psi_\beta^*(r_j) \frac{1}{|r_i - r_j|}\psi_\beta(r_j)\right]\psi_\alpha(r_i) -$$

$$\left[\sum_\beta^{occ} \int dr_j \psi_\beta^*(r_j) \frac{1}{|r_i - r_j|}\psi_\alpha(r_j)\right]\psi_\beta(r_i) = E_i\psi_\alpha(r_i). \quad 3.21$$

Where:

$\left[-\frac{1}{2}\nabla_i^2 + \sum_K^n \frac{1}{|R_K - r_i|}\right]\psi_\alpha(r_i)$, is the T_e (kinetic energy) and potential due to the interaction between electrons and the collection of atomic nuclei.

$\left[\sum_\beta^{occ} \int dr_j \psi_\beta^*(r_j) \frac{1}{|r_i - r_j|} \psi_\beta(r_j)\right]\psi_\alpha(r_i)$, is the coulombic electron-electron interaction also called the Hartree potential.

$\left[\sum_\beta^{occ} \int dr_j \psi_\beta^*(r_j) \frac{1}{|r_i - r_j|} \psi_\alpha(r_j)\right]\psi_\beta(r_i)$, is the Fock or exchange term due to the Pauli principle in the anti-symmetric nature of the interaction given by the second part of the equation. The slater-determinant energy equation is considered best if it can minimize the expected value of the Hartree-Fock Hamiltonian through the variation principle given by the equation:

$$E_{HF} = \psi_{MIN}[\langle\psi|T + V_H + V_X + V_{ext}|\psi\rangle]. \qquad 3.22$$

The HF methods usually fail to wholly describe the many electron system because it doesn't include the correlational effects. Therefore HF method is improved when combinations of a number of slater determinants are used. However, a complete basis-set for such wave-function is very involving.

3.5 Kohn-Sham Equations

Kohn-Sham proposed the following approach to approximate the functional in many–body electron system. They considered an auxiliary system of non-interacting electrons moving in an external potential V^{ks} but whose ground state electron density was the same as that of a real interacting system with kinetic energy and the electron density are known exactly from the orbitals. In the non-interacting system, the universal functional is given by,

$$F[n(r)] = T_s[n(r)] = \langle\varphi^{ks}|T|\varphi^{ks}\rangle. \qquad 3.23$$

And the total energy functional is expressed as

$$E^{ks}\left[n(r) = min\left|T_s\big(n(r)\big) + \int V^{ks}(r)n(r)dr - \mu\right| \int n(r)\acute{d}^3r - N\right|\right]. \quad 3.24$$

Where μ is the Lagrange multiplier which ensures that the total number of electrons is conserved. The function V^{ks} can be determined as follows:

From the interacting system, we have the universal functional as

$$F[n(r)] = T_s[n(r)] + E_H[n(r)] + E_{XC}[n(r)]. \quad 3.25$$

At the ground state,

$$O = \frac{\delta E_{GS}}{n} = \frac{\delta T_s}{\delta n} V_H(r) + V_{xc} + V_{ext}(r) - \mu. \quad 3.26$$

Similarly, for the Kohn-Sham equation at the ground state,

$$O = \frac{\delta E_{Gs}^{ks}}{\delta n} + V^{KS}(r) - \dot{\mu}. \quad 3.27$$

We can now obtain the Kohn-Sham potential from the equations 3.26 and 3.27

$$V^{KS}(r) = V_H(r) + V_{xc}(r) + V_{ext}(r). \quad 3.28$$

This is the definition of the KS potential. The KS self-consistent equations can be expressed as

$$\left[-\frac{\hbar^2}{2m}\nabla^2 + V^{KS}(r)\right]\psi_i^{KS}(r) = \epsilon_i \psi_i^{KS}(r). \quad 3.29a$$

$$V^{KS}(r) = V_{ext}(r) + V_H(r) + V_{xc}(r). \quad 3.29b$$

$$n(r) = \sum_{i\epsilon occ}\left|\psi_i^{KS}(r)\right|^2. \quad 3.29c$$

Where: $V_H(r), V_{ext}(r)$and $V_{xc}(r)$ are Hartree potential, external potential acting on the particles and the exchange correlation potential respectively. $V_H(r)$, and $V_{xc}(r)$ are expressed as,

$$V_H(r) = \int \frac{n(\acute{r})}{|r-\acute{r}|} d. \qquad 3.30a$$

$$V_{xc} = \frac{\delta E_{xc}(n(r))}{\delta n(r)}. \qquad 3.30b$$

These equations are nonlinear and therefore need to be solved self-consistently. The main challenge in this is on the E_{xc} term called the exchange correlation energy .Its explicit form is unknown.

3.6 Exchange-Correlation Approximations

This is a very crucial quantity in the Kohn-Sham approach expressed as a functional of the density $E_{xc}[n]$. It is the difference between the exact total energy of a system and the classical Hartree energy (Ngeywo, 2016). In this definition the kinetic energy is non-interacting.

$$\mathrm{E_{XC}(n) = T(n) - T_o(n) + U_{XC}} \qquad 3.31$$

Where: $T(n)$ is the exact kinetic energy function, $T_o(n)$ is the non-interacting kinetic energy and U_{xc} is the interaction of the electrons with their own exchange-correlation hole. Applying the classical electrostatics interaction between the electron density $n(r\ )$ and the whole density $E_{xc}(r, \acute{r})$ we have

$$E_{XC}[n(r)] = \frac{1}{2} \iint dr d\acute{r} \frac{[n(r) n_{xc}(r,\acute{r})]}{|r-\acute{r}|}. \qquad 3.32$$

From this equation E_{XC} is unknown and thus approximation functional based upon the electron density are introduced to describe the term.

3.7 Density Functional Theory (DFT)

Densities of particles in their ground state for quantum many-body system, is well described in modern DFT (Hohenberg P, 1964). Density is taken as a fundamental variable in all the properties of the system and can be a unique functional of ground state density. Ground state energy is used to determine the Hamiltonian (H). In principle, the wave-function (φ) of a given state is determined through solving Schrödinger equation with the Hamiltonian (Sahni, 1995). For a one electron moving in a potential $V_{(r)}$ Schrödinger equation becomes

$$H\varphi = E\varphi. \qquad 3.33$$

Where E is eigenvalue of the system, substituting Hamiltonian, H in equation (3.1.1) gives;

$$\mathrm{H} = \left[\frac{\hbar^2}{2m}\nabla^2 + V(r)\right]\varphi(r) = E\varphi(r). \qquad 3.34$$

For a number of electrons (many-body system), the Schrödinger equation is written as;

$$\left[\sum_i^N \left(\frac{\hbar^2}{2m}\nabla^2 + V(r_i)\right) + \sum_{i<j} U(r_i; r_j)\right]\varphi(r_1, r_2, \dots\dots\dots r_N) = E\varphi(r_1; r_2, \dots\dots\dots r_N). \qquad 3.35$$

Where N is the total number of electrons and $U(r_i; r_j)$ is the electron-electron interaction. The system can be specified by choosing V(r), and substituting in the Schrödinger equation. This solves the equation for the wave function and also used to calculate the observables (Tong & Chu, 1997). One of particles solved in this manner is the particle density. Potential V(r) can be expressed in terms of electron density as:

$$\hat{\hat{V}} = \int d^3\, rV(r)\hat{\hat{n}}(r). \qquad 3.36$$

Equation (3.36) gives expectation value of $\hat{\hat{V}}$;

$$\langle \psi\, |\hat{V}|\, \psi \rangle = \int d^3\, rV(r)\hat{n}(r). \qquad 3.37$$

From this equation charge density can be written as:

$$\mathrm{n(ri)} = \langle \psi\, |\hat{n}\, (ri)|\, \psi \rangle \;\; = \mathrm{N} \int d^3 r_2 \int d^3 r_3 \ldots . \int d^3\, rN\, \psi^{*}(r_1, r_2 \ldots .. r_N)\, \psi$$

$$(r_1, r_2 \ldots \ldots, r_N) \qquad 3.38$$

There are basically different types of DFT methods. Some of these methods are discussed as follows.

3.7.1 Local Density Approximation

The local density approximation (LDA) is among most significant functions that were proposed by Hohenberg and Kohn in early 1960s. It was ideally to approximate the exchange-correlation energy locally (Perdew, *et al.,* 2014) $\mathrm{E_{XC}}$ [n(r)], of an interacting electron system by the exchange-correlation energy of homogeneous electron gas of density$\rho(r)$,

$$\mathrm{E_{xc}^{LDA}}[\rho(r)] = \int \rho(\mathrm{r})\varepsilon_{xc}\rho(\rho)\mathrm{dr}. \qquad 3.39$$

Where, $\varepsilon_{xc}\rho$ is the exchange-correlation energy per particle of a uniform electron gas density. The exchange-correlation potential is expressed as;

$$\mathrm{V_{xc}^{LDA}}[\rho(\mathrm{r})] = \frac{\delta E_{xc}^{LDA}}{\delta\rho(r)} = \epsilon_{xc}(\rho) + \rho(r)\,\frac{\delta\epsilon_{xc}(\rho)}{\delta\rho}. \qquad 3.40$$

For practical use of LDA in calculations, it is necessary to determine the exchange-correlation energy for a uniform electron gas of a given density. $\epsilon_{xc}(\rho)$ Which can be substituted into exchange and correlation potentials as:

$$\epsilon_{xc}(\rho) = \epsilon_x(\rho) + \epsilon_c(\rho). \quad 3.41$$

LDA is the oldest exchange-correlation function with many weaknesses. It predicts high binding energies, bond length and lattice constants of semiconductors

3.7.2 Generalized Gradient Approximation

Development of generalized gradient approximation (GGA) exchange-correlation functional was as a result of an assumption made by Hohenberg and Kohn that LDA wouldn't work in real systems. GGA accounts for non-uniformity of the electron density. It is expressed as

$$E_{xc} = E_{xc}[\rho(r), \nabla\rho(r)]. \quad 3.42$$

WhereE_{xc} define the exchange correlation energy. The advantage of GGA is that it estimates better results when predicting the molecular geometries and ground-state energies, though computationally more expensive compared to LDA. GGA is also reliable for predicting magnetic properties of 3d transition metals.

Despite all that success GGA is limited in predicting lattice parameters and does not accurately treat hydrogen-bond. More advanced and probably more accurate than the GGA functional are the new meta-GGA functional like the ones parameterized by Tao-Perdew-Staroverov-Scuseria (TPSS)

3.8 Van-der-Waals Interaction

Van der Waals (VdW) is intermolecular forces just like covalent and metallic bonds that exist in some compounds. Though weak, they are always attractive, and purely quantum forces that exists between every two or more fragments of matter. Van der Waals interactions balances with electrostatic and exchange repulsion interaction and together they control the packing of crystals, orientation of molecules on the surface

and formation of the structure among others. In calculating the cohesive energy of layered materials, VdW must be considered (Bu, *et al.,* 2013). In treatment of van der Waals in DFT, the total energy of the system is expressed as

$$E_{DFT-disp} = E_{KS-DFT} + E_{disp}. \quad 3.43$$

Where; $E_{DFT-disp}$ is the normal self –consistent Kohn-Sham energy and E_{disp} is dispersion correction. There are two common methods of solving for VdW in DFT. They include Grimme DFT-D2 (Grimme, 2006) and Tkatchenko and scheffle methods (TS) (Bu, *et al.,* 2013). In DFT-D2, in order to avoid near-singularities for small interatomic distances, a dumping function (f_{dmp}) must be employed;

$$f_{dmp}(R_{ij}) = \frac{1}{1+e^{-d\left(\frac{R_{ij}}{R_r}-1\right)}}. \quad 3.44$$

Where; R_r is the sum atomic VdW radii. However, in TS method, dispersion coefficients and damping function are charge-density dependent. As a result, .it is able to account for variations in VdW contribution of atoms due to their local chemical environment, in this study we have employed DFT-D2 method for VdW contribution in the bulk system.

3.9 Plane waves

In computational modeling of solids, unit cell are defined as $\tilde{a}, \tilde{b}, \tilde{c}$ where arrangement of atoms is in regular repeating pattern. Thus in the nuclei the periodical arrangement of repeating pattern has periodic lattice potential $u_{(r)}$ acting on the electrons. As such the single Schrödinger equation under periodic potential $u_{(r)}$ is written as

$$\left(\frac{-1}{2}\nabla^2 + u_r\right)\varphi = \in \varphi. \quad 3.45$$

The Bloch theorem states that the one electron wave function obeys the equation

$$\varphi_{i,k}(r) = exp^{ik.r}\mu_{k(r)}. \quad 3.46$$

Where: $\mu_{k(r)}$has the periodicity of the lattice potential acting on the electrons. This allows the plane wave expansion of the electron wave function,

$$\varphi_{i,k(r)} = \sum_G c_i\, k + G e^{i(k+G)}r. \quad 3.47$$

Where; G is the reciprocal lattice vector. The Kohn-Sham equations in the K space then reduce to the following matrix eigenvalue equation,

$$\sum \left\{\frac{1}{2}|k+G|^2\delta GG' + V_{ext}(G-G') + V_H(G-G') + V_{xc}(G-G')\right\} C_i\, k+G =$$

$$\in_i\, C_i k + G. \quad 3.48$$

Where; V_{ext} the static total electron-ion is potential, V_H is the Hartree potential of the electrons, i and ϵ are the Kohn-Sham eigenvalue, V_{xc} is the exchange correlation potential and $C_i k + G$ is the coefficient of plane-wave basis set. In practice not all wave vectors are needed, hence a convergence test is used to establish an appropriate value of parameters under study. Convergence means to optimize the parameters to be used in the Vienna ab initio simulation package (VASP). It is a feature applicable to plane wave basis where accuracy of computation depends on single parameters in preference to others. The parameters that need to be converged are K-point and cut-off energy.

The objective of K-point convergence is to find a sufficient dense mesh for integrating the first Brillion zone. The first 'Brillouin' zone is defined as the Wigner-Seitz cell of the reciprocal lattice described by the planes that are perpendicular bisector between the lattice points and the origin of the reciprocal lattice (Pack & Monkhorst, 1977). Reciprocal lattice gives information about periodicity of lattice in reciprocal units.

Reciprocal space is often used than real space in diffraction to characterize materials. Figure 3.1 shows Brillion zone (BZ) of hexagonal VS_2 (Curtarole, *et al.*, 2012) along high symmetry points (Γ-M-K-Γ-A-L-H-A-L-M-K-H), where $\tilde{a}, \tilde{b}, \tilde{c}$ represent reciprocal lattice vectors.

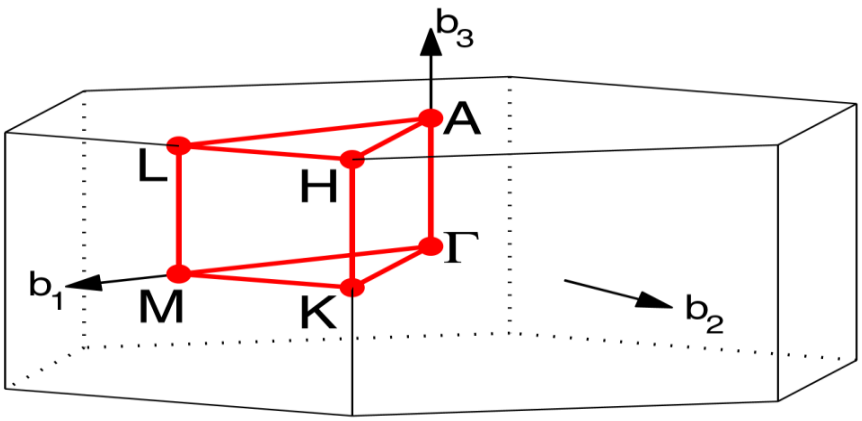

Figure. 3. 1: Brillion zone (BZ) of hexagonal VS_2

3.9.1 K-point Convergence

Brillouin zone was sampled using Monkorst Pack method (Monkhorst & Pack, 1977) denoted as $n_1 \times n_2 \times n_3$ grids which results in a total number of k-points presented as $n_1.n_2.n_3$. This implies that the computational cost heavily relies on the total number of k-points. Dense grid requires more central processing unit (CPU) time than a less dense grid. Figure 3.2 shows the convergence of K-point (x=y), axis in the bulk VS_2

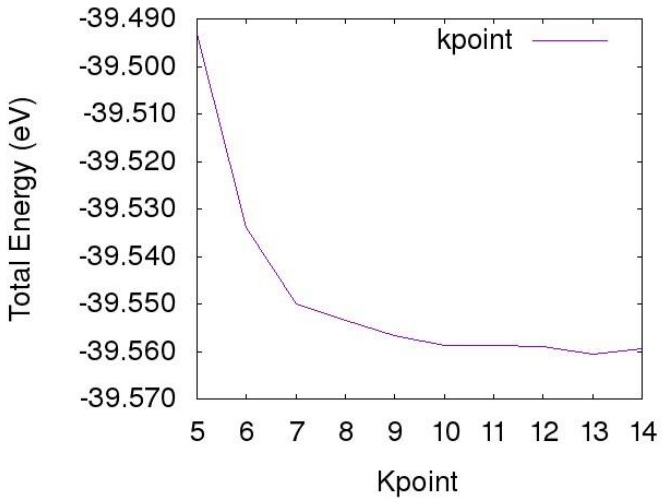

Figure 3.2: Total Energy versus K-point for VS_2

In this work, we used a K-point grid of 12 12 5 for the bulk VS_2 and 3 3 1 for the supercell

3.9.2 Cut-off Energy Convergence

The cut–off energy in (eV) for the plane wave basis is a significant parameter in DFT calculation. The convergence of the cut-off energy with respect to total energy is evaluated at a fixed k-point mesh in the KPOINT file and experimental lattice parameter obtained from the existing material project database. For this case cut-off convergence is as shown in the Figure 3.3

As one can see a cut-off of below 500eV was insufficient. Therefore, one can choose values above the default cut-off energy (550eV) in order to obtain accurate results. High energies are undesirable since they only increase the computational cost without improving the accuracy.

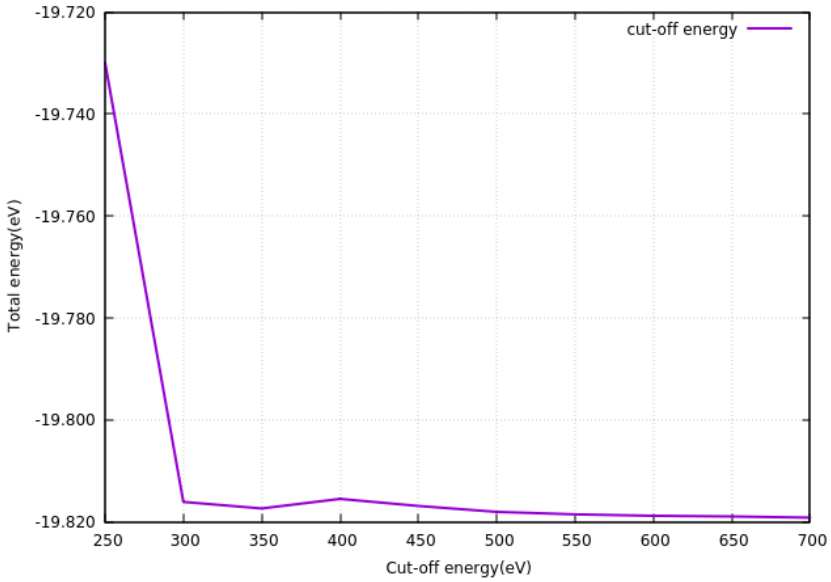

Figure 3.3: A graph of cutoff energy against total energy for VS_2

The graph indicates that (520eV) is indeed the minimum value for cut-off energy that will give reasonable results. However, any energy above 550eV is sufficient for any calculations though it is time consuming.

CHAPTER FOUR

METHODOLOGY

4.1 Introduction

All properties were characterized via *ab initio* calculation with the density functional theory (DFT) .DFT calculations were carried out with VASP (Hafner, 2008) which is based on the Kohn-Sham DFT (KS-DFT) (Levy & Frouidevaux, 1979) with the GGA parameterized by PBE for exchange correlation functions (Balchin, 1976). Birch-Murnaghan equation of state (EOS) was used during calculation of the cell parameters (Murnghan, 1944). An interaction between ions was described using projector augmented wave (PAW) (Kresse & Joubert, 1999) of minimize the van der Waals forces action between the layers of the bulk VS_2 system, Grimme DFT+D2 (Grimme, 2006) correction method was employed. The Brillion zone was sampled using a set of 12x12x2, gamma centered k-mesh for the structural optimization.

4.2 Structural Properties.

The relative stability, cohesive energy volume optimization and lattice constants were determined by fitting the volume energies in the Birch-Murnaghan equation of state (EOS). Equation of state is a constitutive expression that gives a mathematical relationship between two or more state variables associated with a material. This variable includes: internal energy, volume, pressure, temperature among others. In this study third order Birch-Murnaghan equation of state that was used is based on Taylor series expansion of pressure in terms of Eulerian strain (f). It is a partial derivative of internal energy with respect to volume at constant temperature. At

absolute zero the entropy of a system is constant, so that the thermodynamic identity is the change in energy accompanying a change in volume. This can be written as

$$P = -\frac{\partial E}{\partial V} \qquad 4.1$$

Applying chain rule the expression of pressure can be written as

$$P = -\left(\frac{\partial E}{\partial f}\right)\left(\frac{\partial f}{\partial V}\right) \qquad 4.2$$

This can be written in terms of bulk modulus and Eulerian strain as

$$P(f) = 3\beta_{\circ} f(1+2f)^{\frac{5}{2}}\left[1 + \frac{3}{2(\acute{\beta}_{\circ}-4)f} + \cdots\right] \qquad 4.3$$

Eulerian strain is expressed in terms of reference and equilibrium volume as:

$$f = \frac{1}{2}\left[\left(\frac{V}{V_O}\right)^{\frac{-2}{3}} - 1\right] \qquad 4.4$$

Substituting equation 4.4 to 4.3 we

$$P(V) = \frac{3}{2}\beta_O\left[\left(\frac{V_O}{V}\right)^{\frac{7}{3}} - \left(\frac{V_o}{V}\right)^{\frac{5}{3}}\right]\left\{1 + \frac{3}{4}\left(\grave{\beta}_o - 4\right)\left[\left(\frac{V_o}{V}\right)^{\frac{2}{3}} - 1\right]\right\} \qquad 4.5$$

Where: V_o is the equilibrium volume, V is the reference volume, β_o is the bulk modulus and $\acute{\beta}_o$ is the derivative of bulk modulus. Bulk modulus is proportional to the curvature of the equation of state at the equilibrium volume. Together with its derivative they are higher order function related as

$$\beta_0 = -V\left(\frac{\partial P}{\partial V}\right)_{V=V_0} = V\left(\frac{\partial^2 E}{\partial^2 V}\right)_{V=V_0} \qquad 4.6$$

$$\acute{\beta}_0 = \left(\frac{\partial \beta_0}{\partial P}\right)_{V=V_0} = \frac{\partial}{\partial P}\left(V\frac{\partial^2}{\partial V^2}\right)_{V=V_0} \qquad 4.7$$

Bulk modulus is a coefficient of elasticity of a substance that is expressed as the ratio between pressure that acts to change the volume of the substance and the fractional

change in volume produced (Garai, 2007), while the derivative of the bulk modulus is a dimensional parameter. For *ab initio* study, energy is expressed as a function of volume as follows

$$E(V) = E_o + \frac{9V_o\beta_O}{16}\left\{\left[\left(\frac{V_o}{V}\right)^{\frac{2}{3}} - 1\right]^3 \acute{\beta}_o + \left[\left(\frac{V_o}{V}\right)^{\frac{2}{3}} - 1\right]^2 \left[6 - 4\left(\frac{V_o}{V}\right)^{\frac{2}{3}}\right]\right\} \qquad 4.8$$

V_0 , is the equilibrium volume under study. In this work structural stability were determined full relaxation calculations of volume, shape and atomic position was performed while keeping the lattice type constant. Self-consistent calculations at different volume each predicting equilibrium volume was then carried out. A third order Birch-Murnaghan equation of state (EOS) was then fitted to the obtained energies in which the initial structure was subjected to uniform scaling resulting in thirteen volumes. At each volume, partial relaxation was done, whereby, atomic positions and cell shapes were allowed to relax at a constant volume (Bucko, *et al.*, 2005)

4.3 Electronic properties

The electrical conductivity of conductors, semiconductors and insulators is explained using the energy band theory. Electrons/ions in solids are the main charge carries. In any given atom, electrons are arranged around the nuclear in what we call orbitals. According to the energy-band theory, when two are more orbitals overlaps, they result in some energy bands being occupied fully while others unoccupied. The more occupied bands are called valence bands and the unoccupied one are called conduction bands. Between these distinct bands region some bands may be left empty depending on the overlap which leads to a region called band gap. The band gap is majorly used in the classification of materials as conductors, semiconductors and insulators.

Insulators have a band gap of more than 3eV while that of semiconductors is smaller. Metals do not have a band gap and their conduction band is partially filled.

Band structure calculations take advantage of the periodic nature of a crystal lattice, exploiting its symmetry. The single-electron Schrödinger equation is solved for an electron in a lattice-periodic potential, giving Bloch waves as solutions:

$$\varphi_{nk}(r) = e^{ik.r}\mu_{nk}(r) \qquad 4.9$$

Where: **k** is called the wave vector. For each value of **k**, there are multiple solutions to the Schrodinger equation labeled by *n*, the band index, which simply numbers the energy bands. Each of these energy levels evolves smoothly with changes in **k**, forming a smooth band of states. For each band we can define a function $E_n(\mathbf{k})$, which is the dispersion relation for electrons in that band. The wave vector takes on any value inside the Brillouin zone, which is a polyhedron in wave vector space that is related to the crystal's lattice. Wave vectors outside the Brillouin zone simply correspond to states that are physically identical to those states within the Brillouin zone. The density of states (DOS) represent the number of states which can be occupied at each energy level. In energy range$[E, E + dE]$, the DOS per unit volume is given as

$$N(E) = \frac{\Omega}{2\pi^3}\int_{BZ}^{i} dk\ \delta\left(E_{i,k} - E\right) \qquad 4.10$$

To get the contribution of a given atom to each state, projected density of states is used (PDOS).

In this study, electronic properties were investigated by analyzing the band structure and the density of state (DOS) using the PBE exchange correction potential. This was

necessary to explain the electrochemical performance of electrodes. Self-Consistent was first calculated to get a well converged charge density. This was then followed with a non-self-consistent calculation in co-operating the already converged charge density. The high symmetry K-point path (Γ-M-K-Γ) was used to get a well converged DOS.

4.4 Gravimetric Capacity

Gravimetric capacity is the measure of the total charge capacity stored by the battery per gram of the battery's weight. Batteries are specified by three main characteristics: chemistry (which includes lead, nickel and lithium), voltage (marked as nominal voltage) and capacity (which represent specific energy in Ampere-Hours). The capacity of battery is determined by the amount of Li ion stored by the battery. VS_2 was therefore investigated in this section in order to determine the capacity of the battery. First optimization of the available space to accommodate the Li ions was carried out. A supercell of 4x4x1 was adopted in order to avoid interaction between two Lithium atoms and the structure visualized in VESTA before further calculations were done. The pure Vanadium Sulphide supercell has one Vanadium atom surrounded by three Sulphur atoms.

The theoretical capacity of a cell is therefore calculated as per the following equation (Hasa, 2015)

$$Q_{the} = \frac{nF}{3600 \times Mw} \qquad 4.11$$

Where: *n* is the number of charge carries, F is the Faraday constant and Mw is the molecular weight of the active material used in the electrode. From the above equation *n* is the only variable in the determination of the capacity of the anode material. The

binding energy was calculated by varying the value of *n* from minimum to maximum. By the following equation the adsorption energy (Jing, *et al.,* 2013)

$$E_{ads} = \frac{(E_{total} - E_{substrate} - nE_{Li})}{n} \qquad 4.12$$

Where: E_{ads} is the adsorption energy, E_{total} is the total energy of VS_2 and Li, $E_{substrate}$ is the energy of pure VS_2 and E_{Li} is the chemical potential of Lithium i.e the cohesive energy per atom of bulk Li. A number of configurations with stoichiometry of Li_xVS_2 were first constructed where *n* lithium atoms were placed in different sites of the substrate followed by full geometry optimization.

CHAPTER FIVE

RESULTS AND DISCUSSION

5.1 Structural Stability

Calculation of the structural energetic parameters were done using both the PBE and PBE+D2 functions. Since VS_2 is a layered material, PBE could not give accurate results because it is non inclusive of the van der waals forces.

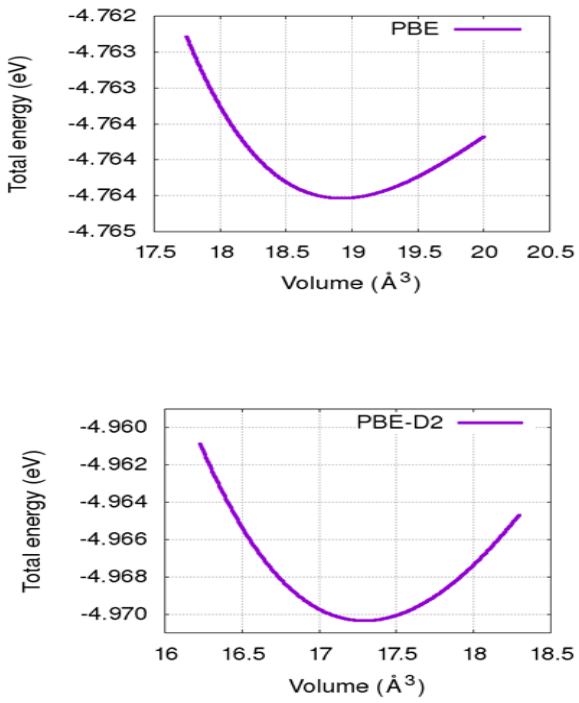

Figure 5.1: Total energy against volume fitted to the third order Birch-Murnaghan equation of state plots for both PBE and PBE-D2.

Therefore PBE-D2 function was employed especially when working with the bulk structure of VS_2. Including the van der waals term helps account for the interlayer attractions that dominates by van der waals forces in the bulk structure. From figure 5.1 above, the equilibrium volume obtained by PBE shifted to the right while PBE-

D2 the value shifted to the left. Other information extracted from the EOS fits are summarized in the table 5.1. The computed structural parameters were comparable to experimental values Gauzzi, *et al.*, 2014) as well as other computational values (Natalia, *et al.*, 2017). From the data though PBE predicted well the in-plane cell parameters (3.179 Å), it overestimates the out of plane values (6.487 Å) which translate to higher volume (56.77 $\mathbf{Å}^3$) as compared to experimental value (51.59 $\mathbf{Å}^3$).

Table 5.1: Tabulated results of the bulk and monolayer structural properties computed with PBE and PBE-D2.

Crystal	Functions	Results.	a=b (**Å**)	c (**Å**)	V-S-V bond angle	E_{coh} (eV)	V-S distance (**Å**)	Vol ($\mathbf{Å}^3$)
BULK								
H-phase	PBE	Calculated values	3.179	6.487	84.44	-4.76	2.25	56.77
	PBE-D2	Calculated Value	3.168	5.835	85.78	-4.97	2.35	50.71
		Other DFT values	3.16	5.79	85.06	-4.96	2.33	50.07
		Experimental	3.23	5.71	`-	-	-	51.59
	MONOLAYER							
	PBE	Calculated Values	3.17		84.43	-4.96	2.36	
		Other DFT values.	3.181		84.44		2.351	

PBE+D2 underestimates both in-plane (3.168 Å) and out-plane (5.835 Å) lattice constants and this also automatically translates to its volume being low (50.71 $Å^3$) compared to experimental value (51.59 $Å^3$). For the monolayer slap, PBE function was used all through since the effect of van der waals force is negligible.

The stability of VS_2 basing on the basis of the cohesive energy was also analyzed. The more negative cohesive energy indicates that the system is stable upon decomposition. From table 5.1, all the cohesive energy obtained were both negative irrespective of the function used. This shows that the hexagonal VS_2 is stable upon decomposition into its constituent atoms. The more negative cohesive energy value (-4.97eV) for bulk system is achieved with PBE-D2 due to the inclusion of van der waals. The value is close to the monolayer results (-4.96eV)

5.2 Density of State

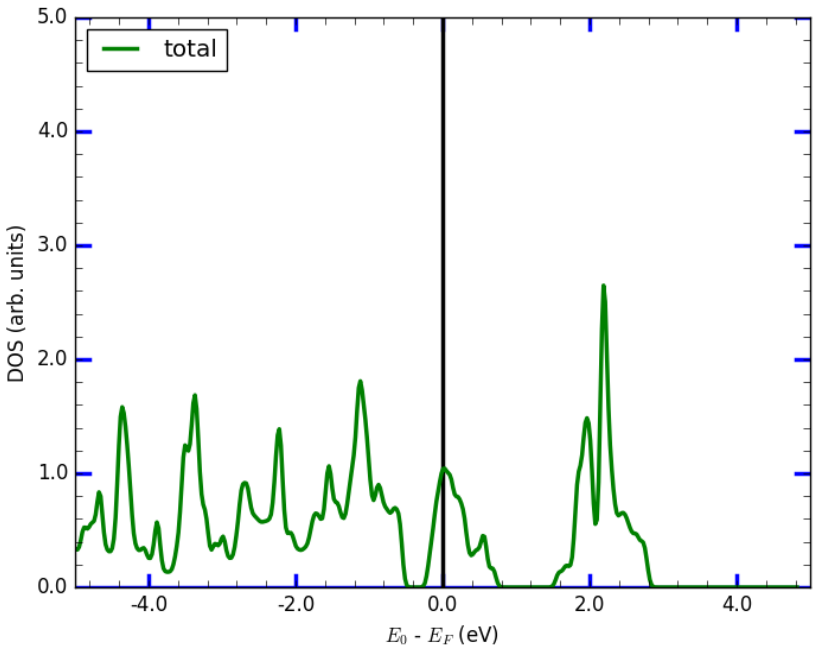

Figure 5.2: Graphical representation of density of states of pure vanadium disulphide.

The density of state (DOS) of VS_2 with and without lithium adsorbed was computed for the monolayer slap by employing PBE function since it predict better structural results in the monolayer state. Figure 5.2 the DOS for pure VS_2 shows the metallic state of VS_2 with a number of electronic states at the Fermi level

Figure 5.3 shows the DOS plots for VS_2 adsorbed with lithium atoms where the metallic state is still maintained.

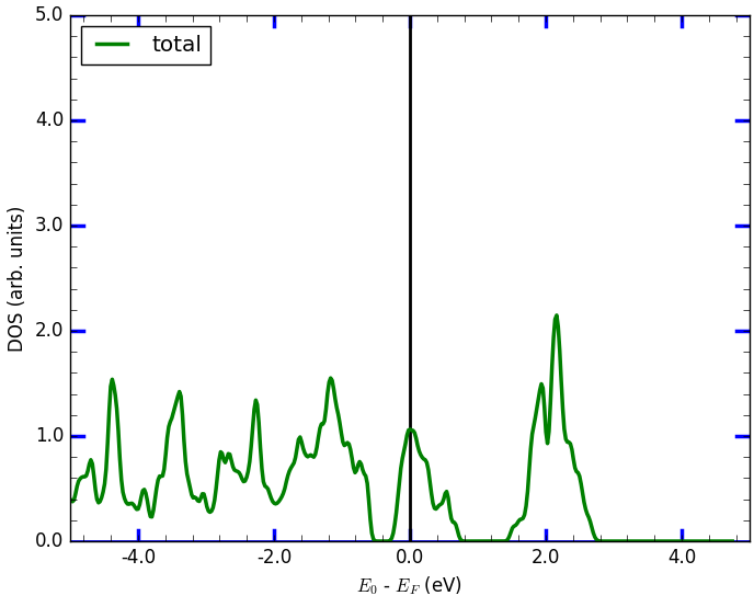

Figure 5.3: Graphical representation of density of state of vanadium disulphide adsorbed with single lithium atom at the V-site.

The difference between the two plots is indicated by the difference in the energy picks. The energy orbitals with longer picks are deep energy orbitals in relation to shorter ones. The lithium adsorbed VS_2 plot shows deep energy orbitals then pure VS_2. The increase in the orbital energy is contributed with the addition of lithium atoms.

5.3 Band Structure

To investigate the allowed and forbidden band gaps of VS_2, band structure calculation was done for both pure and lithium adsorbed VS_2. The first calculation was done to

get an already converged charge density. The converged charge density was then used in the non-self-consistent calculation. The bands characteristic at the conduction and valence regions are used in categorizing a system. For insulators the conduction and valence band are separated by a wide band gap such that the electrons cannot move from the valence band to conduction band while for semiconductors the band gap is narrow and on slight excitation the electron can move from valence band to conduction band. Metals do not have a band gap and hence the conduction and valence bands overlap.

In this study the Fermi level was shifted to zero and the conduction band minimal crosses over to the valence band as shown in the figure 5.4.

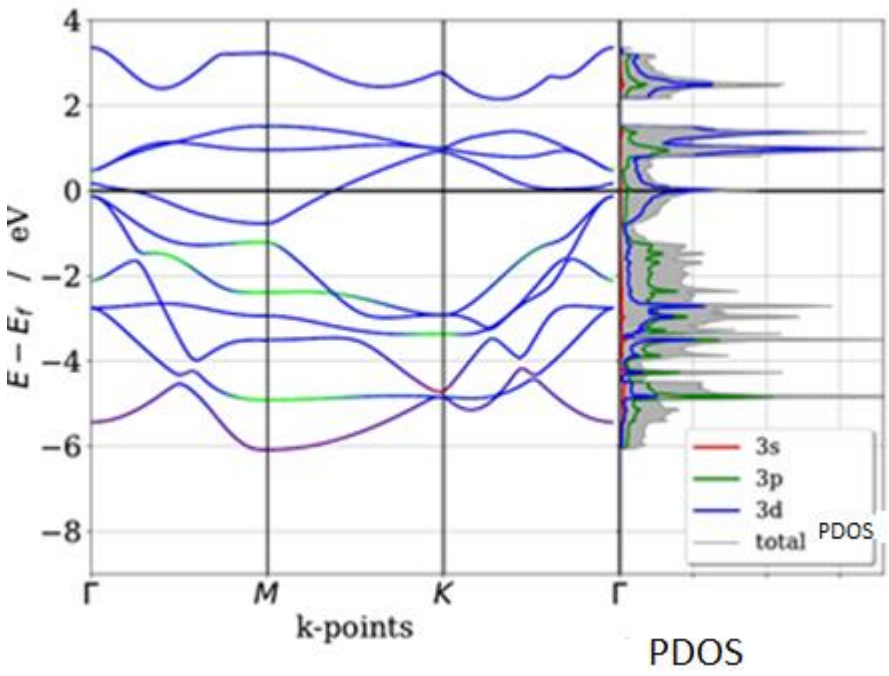

Figure 5.4: Bands and PDOS for VS_2. At the Fermi level, the emergence of PDOS is contributed by both Vanadium (V-3d) and Sulphur (S-3p) states for pure VS_2

This indicates that monolayer VS_2 is metallic. The single bands in the conduction bands shows the non-bonding state while in the valence bands we have the bonding states. VS_2 also experience degeneracy due to the crystal field.

The metallic state is contributed by V-3d and S-3p as incised by the PDOS. At the ferm level vanadium V-3d is domited as compared to sulphur S-3p. sulphur S-3s is very low in energy thus no much contribution at the fermi level. This results are also in line with other theoritacl work as shown in Fig 5.5. Also a slid deference in the peak maybe as a result of defferent methodology.

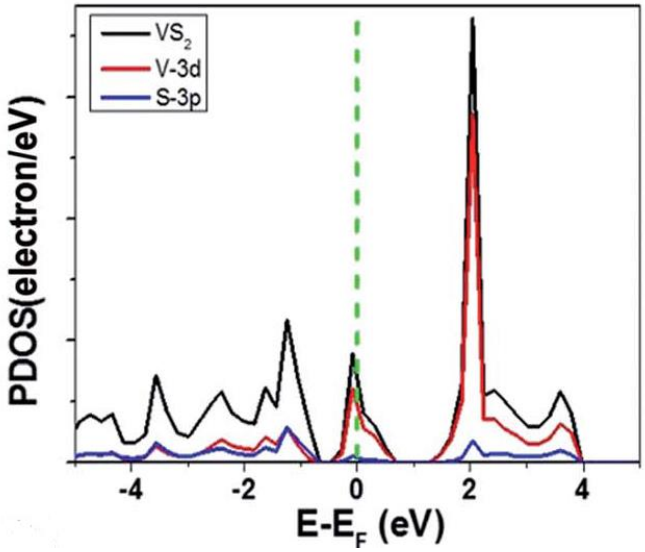

Figure 5.5: PDOS for VS_2, V-3d and S-3p (Wenhui, et. al., 2016)

5.4 Gravimetric Capacity

From calculations there are three possible sites for Li adsorption on VS_2 monolayer. The available adsorption sites are V-site (on top of vanadium atom), S-site (just above the sulphur atom) and the H-site (At the center of each hexagonal V-S-V-S-V-S-V shape).

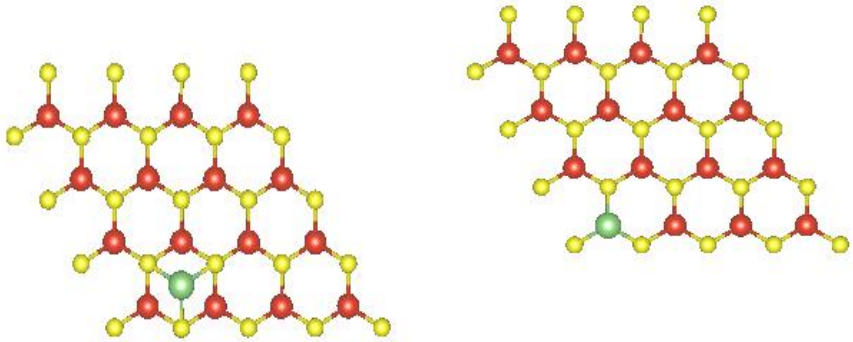

(a) (b)

Figure 5.6: Top view of (a) H-site and (b) V-site adsorption. Lithium atom represented by the green ball, the lithium atom forms covalent bond with three Sulphur atoms around it.

The S-site (just above the S atom) is not local minimum for adsorption since the Lithium atom moves to the V-site after relaxation (Yu, *et al.*, 2014) thus it was not considered in this calculation.

5.4.2 Adsorption Energy.

The capacity of the battery is also determined by the reversible reaction between the host electrode and the Li-ions which is given by the following equation

$$\mathbf{Li_nVS_2} \rightleftharpoons \mathbf{VS_2 + nLi} \quad -\Delta\mathbf{E} \qquad \mathbf{5.1.}$$

The $\Delta \boldsymbol{E}$ value is a negative value indicating the reaction is exothermic. A favorable reversible reaction is the one with the more negative reaction energy. Lithium atoms we adsorbed on the different side of the VS_2 as shown in fig 5.8 below and the adsorption energy calculated at each stage

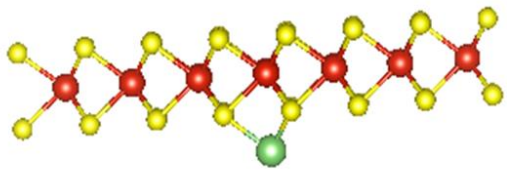

(a)

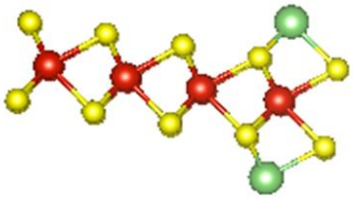

(b)

Figure 5.7: Schematic illustration of the (a) single lithium ion, (b) double lithium ions adsorption on V-site the green ball represents lithium ion while the yellow and maroon are the vanadium and Sulphur atoms respectively.

The values tabulated in table 5.2 were arrived at after fitting different energy values in the equation 4.8. From this equation different values of the energy are achieved by varying the value of *n* where *n* is an integer. The resultant adsorption energy value must be negative all through in order to maintain the state of the reaction that is exothermic.

Table 5.2: Tabulated results of adsorption energies, Li-V and Li-S bond length for the possible insertion sites of Li-ion on monolayer VS_2

n Lithium ion		Active sites	Adsorption energy (eV)	Li-V distance(Å)	Li-S distance(Å)
1	Calculated	H	-1.91	3.51	2.38
	Other DFT	H	-2.01	_	2.44
	Calculated	V	-2.00	3.00	2.38
	Other DFT	V	-2.13	_	2.42
2	Calculated	V	-1.96		

The V-site is the most favored site with more negative adsorption energy. This indicates a more favorable reaction occurring between VS_2 and lithium ions.

Our calculations indicate when one Lithium ion is adsorbed on the surface of VS_2, the adsorption energy at the V-site (-2.00eV) has the lowest potential energy compared to the H-site (-2.01eV). These results are in line with other reported DFT calculations (-2.13eV) (Wenhui, et al., 2016). Thus the more favorable adsorption monolayer site is the V- site. We therefore proceeded with the V-site by adsorbing two lithium atoms.

From the results (adsorption energy of -1.96eV) it is also clear that VS_2 monolayer can provide a negative binding energy even when double lithium atoms are used. From the trend above, increasing the number of lithium atoms the energy values tend to be positive. The reaction will become endothermic (positive binding energy values).

The gravimetric capacity was then calculated by fitting the value of *n* in equation 4.7 when is substituted by *n=2* the total gravimetric capacity was found to be *466mAh/g.*

In comparison to other TMDs for instance MoS_2, which can also store lithium ions up to Li_2MoS_2, the capacity is *335mah/g* (Jing, Zhou, *et al.*, 2013). This is lower than that of VS_2, this is due to high molecular weight of MoS_2. From this we can conclude that VS_2 monolayer as a host electrode material boosts the capacity of Li-ion battery.

CHAPTER SIX

CONCLUSION AND RECOMMENDATION

6.1 Conclusions

Naturally vanadium is a transitional element with its valence electron in the d-state. It is less electronegative element which leads to ionic bond with Sulphur. Both Sulphur and vanadium atoms are viable for battery application. The results indicate that both bulk and H-phase monolayer VS_2 of crystal number of 1013525 and space group 194 are stable at room temperature maintaining the hexagonal structure. The lattice parameters calculated were a=b 3.18 Å, c=5.935Å for 3D and a=b 3.17Å for 2D. The cohesive energy was found to be -4.75eV thus the compound is stable upon decomposition.

Electronic stability was also investigated on the monolayer VS_2. The pure and lithium adsorbed VS_2 is electronically stable with zero band gap. Thus it exhibits better electrochemical performance as anode material in lithium ion battery.

The binding energy for single and double lithium atoms on the monolayer VS_2 was systematically studied, the results indicates that v-site is the favorable site for adsorption and it accommodates a maximum of two lithium atoms maintaining the exothermic reversible reaction, as a result VS_2 gives a maximum gravimetric capacity of (466mAh/g) in comparison to other studied anode counterparts.

6.2 Recommendation

This study is open for future research in the following areas:

1) The transport and diffusion properties of VS_2 in relation to its applicability an anode material.

2) Use of hybrid functional to confirm the same properties.

3) Experimental test on the application of VS_2 in Li-ion battery.

REFERENCES

Balchin, A. (1976). Growth and the crystal characteristics of dichalcogenides having layer structures in crystallography and crystal of material with layered structures. *springer*, 1-50.

Bu, T., Lebegue, S., Hafner, J., & Angy, J. (2013). Tkatchenko-Sche_er van der Waals correction methhods and without self-consistent screening applied to solids. *Physical Review B*, 064110.

Bucko, T., Hafner, J., & Angyan, G. (2005). Geometry optimazation of periodic systems using internal coordinates. *chemical physical*, 124508-1234509.

Chaofeng, L., Zachary, G., & Guozhang, C. (2016). Understanding electrochemical potentials of cathode materials in rechargeable batteries. *Material matter., 19*, 109-123.

Curtarole, S., Setyawan, W., Hart, G., Jahnatek, M., Chepuldkil, R., Taylor, R., . . . Stokes, H. (2012). Aflow:An automatic framework for hihg throughput material discovery,. *Computational material Science*, 218-226.

Feng, C., Ma, J., Li, H., Zeng, R., Guo, Z., & Liu, H. (2014). *Nano-porous architecture of N-doped carbon nanorods grown on graphene to enable synergetic effects of supercapacitance.*

Feng, J., Sun, X., Wu, C., Peng, L., Lin, C., Hu, S., . . . Xie, Y. (2011). Metallic Few-Layeared VS2 Ultrathin Nanosheets :High Two Dimensional Conductivity for IN-Plane Supacacitors. *American Chemical Society, 33*, 17832-17838.

Garai, J. (2007). *Semi-empirical pressure volume temperature equation of state: MgSiO3 perovskite isan example.* arxiv preprint.

Goodenough, J., & Kim, Y. (2009). Challenges for Rechargeable Lithium Batteries. *Chemistry of materials, 22*, 587-603.

Grimme, S. (2006). Semiempirical GGA-type density fu ctional constructed with a long range dispersion correction. *computational chemisty*, 1787-1799.

Guduru, R., & Leanza, J. (2016). A Brief Review on Miltivalent Intercalation Betteries with Aques Electrolytes. *Nanometerials, 6*, 1189-1192.

Hafner, J. (2008). Ab-initio simulation of materials using VASP:Density-functional theory and beyound. *Computational Chemistry*, 2044-2078.

Hall, P., & Bain, E. (2008). Energy-storage technologies and electricity generation. *ELSEVIER, 36*, 4352-4355.

Hasa, I. (2015). *Researchgate*. Retrieved Augst 16, 2018, from Researchgate: https://www.researchgate.net/post/how to calculate theoritical capacity of a cell.

Hasnain, S. M. (1998). Review on sustainable thermal energy storage technologies, Part I: heat storage materials and techniques. *Energy conservation and management, 39*, 1127-1138.

Hohenberg P, W. K. (1964). Inhomogeneous electron gas. *Phyiscs Reveiw*, 864.

Jian-Zhe, L., & Peng-Fei, G. (2015). VS2 Nanosheets; Apotential Anode Material fro Li-oin Battries. *A Journal of inorganic Materials, 16*, 1338-1339.

Jing, Y., Zhou, Z., Cabrera, C., & Chen, Z. (2013). Metallic VS2 monolayer: a promising 2D anode material for lithium ion batteries. *The Journal of Physical Chemistry C*, 25409-25413.

Kresse, G., & Joubert, D. (1999). From ultrasoft pseudopotentials to the projector augmented-wave method. *Physical Review*, *59*, 1758.

Larramona, G., Choné, C., Jacob, A., Sakakura, D., Delatouche, B., Péré, D., . . . Nagino, M. a. (2006). Nanostructured Photovoltaic Cell of the Type Titanium Dioxide, Cadmium Sulfide Thin Coating, and Copper Thiocyanate Showing High Quantum Efficiency. *Chemistry of Materials 18 (6)*, *3*, 1688-1696.

Levy , F., & Frouidevaux, Y. (1979). Stracural and electrical properties of layerd transition metal selenides. *physics contributional:solid state physics*, 473-474.

Ma, Y., Dai, Y., Guo, M., Niu, C., Zhu, Y., & Huang, B. (2012). Evidence of the Existance of Magnetism in Pristine VX2 Monlayers (X=S,Se) and Their Strain induced Tunable magnetic properties. *American Chemical Socirty*, *2*, 1695-1701.

Maier, J. (2005). Nanoionic : Ion transparant and electochemical Storage in confined system. *Nature material*, 8805-815.

Manyali, G. (2013). *A computational study of layered and superhard carbon-nitrogen material.* johannesburg: Witwatersrand.

Monkhorst , H., & Pack, D. (1977). Special points for brillouin-zone integrations. *physical review*, 5188-5189.

Mueni, M. (2012). *Stractural and Electronic studies of TiO2 and Nb: TiO2 using Density Functional theory.*

Murnghan, D. (1944). The Compressibilty of media under extreme pressure. *national academy of science*, (pp. 244-247).

Natalia, S., Maxim, A., Aleksndr, A., & Zakhar, P. (2017). VS2/Graphene Heterostructures as Promising Anode Material for Li-ion Batteries. *Physical Chemistry*, 24180.

Ngeywo, K. (2016). *Mid-gap states in deffective Anatase TiO2:A Density Functional Theory study plus a Hubbard term(DFT+U).* Eldoret: University of Eldoret.

Nitta, N., Wu, F., Lee, J., & Yushin, G. (2015). Li-ion battery materials: present and future. *materils today, 18*, 252-264.

Pack, J., & Monkhorst, H. (1977). Special points for brilliouin-zone integrations. *physical review*, 1747-1748.

Paier, J., Marsman, M., Hummer, K., Kresse, G., Gerber, C., & Angyan, J. (2006). Screened hybrid density functionals applied to solids. *Chemical physics*, 154709.

Perdew, J. P., Ruzsinszky, A., Sun, J., & Gedanken. (2014). Gedanken densities and exact constraints in density functional theory. *The Jounal of chemical physics, 140(18)*, 533-630.

Placke, T., Kloepsch, R., Duhnen, S., & Winter, M. (2017). Lithium ion, lithium metal, and alternative rechargeable battery. *Journal of solid state, 21*, 1939-1864.

Ponomaranko, L., Schedin, F., Katsnelson, M., Yong, R., Hill, E., Novoselov, K., & Geim, A. (2008). Chastic dirac billiard in graphene quantum dot. *Science*, pg 356-358.

Raji, A., Villeges, S., Fan, X., Silva, G., & Tour, J. (2017). Lithium Batteries with Nearly Maximum Metal Storage. *American Chemical Society*, *11*, 6362-6369.

Sahni, V. (1995). Derivation and reinterpretation of approximation in schrondinger and Hohn-Shown theoryvie a hiererchy within the formalism. *International journal of Quantum Chemistry.*, 591-606.

Tarascon, J., & Armand , M. (2001). Issues and challenges Facing Rechargeable lithium Batteries. *Nature., 414*, 171-179.

Tong, X., & Chu, S. (1997). Density-functional theory with optimized effective potential and self interaction correction for grand states and autoinising resonances. *physical review*, 3406.

Vadim, K., Martin, G., Waldermer, W., Jennnifer, M., Simon, W., Martin, W., & Sascha, N. (2015). Two-dimensional ion chromatography for the separation of ionic organophosphates generated in thermally decomposed lithium hexafluorophosphate-based lithium ion battery electrolytes. *Journal of chromatography, 1409*, 201-209.

Wakihara, M. (2001). Recent Developement in Lithium batteries. *material science and engineering.*, 109-134.

Wenhui, W., Zhongti, S., Wenshuai , Z., Quanping , F., Qi, S., Xudong, C., & Bin, X. (2016). First-principles investigatios of vanadium disulfide for Lithium and Sodium ion battery applications. *Royal Society of Chemistry*, 54874-54879.

Wenpei, F., Yung, B., Peng, H., & Chen, X. (2017). Nanotechnology for multimodal synergistic cencer therapy. *American chemical Society, 117,* 13566-13638.

Wu, X., Jiulin, W., Fei, D., Xilin, C., Eduard, N., Yaohui, Z., & Ji-cuang, Z. (2014). Lithium metal anodes for rechargeable batteries. *Energy & Envinmental Science, 7*, 513-537.

Wu, Z., & Cohen, R. (2006). More accurate generalised gradient approximation for solids. *physics review,* 235115-235116.

Xiao, J., Wang, X., Yang, Q., Xun, S., Liu, G., Koech, K., . . . Lemmon, P. (2016). MoS2 coated hollow carbon spheres for anodes of lithium ion batteries. *Advancet Matter, 3*, 2008-2009.

Xin-Bing, C., Jia-Qi, H., & Qiang, Z. (2018). Review—Li Metal Anode in Working Lithium-Sulfur Batteries. *Journal of The Electrochemical Society, 165*, 6058-6072.

Yu, J., Zhen, Z., Carlos, R., & Zhongfang, C. (2014). Graphene inorganic grapheneanalogs and their composites for lithium ion batteries. *Journal of meterials chemistry, 2*, 12077-12602.

Yu-Guo, G., Jin-Song, H., & Li-Jun, W. (2008). Nanostructred materials for Electrochemical Energy Conversion and Storage Devices. *Advanced material, 117*, 2878-2887.

Zhenguo, Y., Zhang, J., Michael, C., Kitner, M., Lu, X., Daiwon, C., . . . Jan, L. (2010). Electrochemical Energy Storage for Green Grid. *Chemical reviews, 33*, 3577-3613.

Appendix

List of conferences and workshop attended

1) Computational methods in materials science held at Masinde Muliro University of Science and Technology in 2017
2) Computational and theoretical physics annual meeting in 2018 1nd 2019
3) Workshop and planning meeting for Material Science and Solar Energy network for Eastern and Southern Africa (MSSEESA) held at Nakuru -Kenya.

List of papers published

1) Adsorption Energies of Lithium and Sodium Ions on Vanadium Disulphide: A DFT Study.
2) Elastic layer modulus for Janus transitional metal dichalcogenides (in progress).